Catal Lett (2011) 141:1752–1760
DOI 10.1007/s10562-011-0707-y

Selective Aerobic Oxidation of 5-Hydroxymethylfurfural in Water Over Solid Ruthenium Hydroxide Catalysts with Magnesium-Based Supports

Yury Y. Gorbanev · Søren Kegnæs · Anders Riisager

Received: 22 June 2011 / Accepted: 16 September 2011 / Published online: 1 October 2011

Abstract Solid catalyst systems comprised of ruthenium hydroxide supported on magnesium-based carrier materials (spinel, magnesium oxide and hydrotalcite) were investigated for the selective, aqueous aerobic oxidation of the biomass-derived chemical 5-hydroxymethylfurfural into 2,5-furandicarboxylic acid (FDA), a possible plastics precursor. The novel catalyst systems were characterized by nitrogen physisorption, XRPD, TEM and EDS analysis, and applied for the oxidation with no added base at moderate to high pressures of dioxygen and elevated temperatures. The effects of support, temperature and oxidant pressure were studied and optimized to allow a quantitative yield of FDA to be obtained.

Keywords 5-Hydroxymethylfurfural · 2,5-Furandicarboxylic acid · Aerobic oxidation · Ruthenium hydroxide catalysts

1 Introduction

Biomass is a viable feedstock for production of both chemicals and novel fuels, which eventually can replace crude oil and gas (fossil feedstocks) as major raw materials [1]. 5-Hydroxymethylfurfural (HMF) is a product of the dehydration of hexose carbohydrates obtained from lignocellulosic biomass by, e.g. enzymatic hydrolysis [2, 3].

HMF can be readily oxidized to different potentially important products, such as maleic anhydride [4], 2,5-diformylfuran (DFF) [5, 6], 2,5-furandicarboxylic acid (FDA) (Scheme 1) or its dimethyl ester [7–11]. FDA has been established by the US Department of Energy (DOE) biomass program as one of the 12 chemicals that in the future can be used as chemical building block from biomass in biorefineries [12, 13]. In particular, the two carboxylic groups present in FDA make it a valuable polymer building block and hence a possible renewable alternative to terephthalic, isophthalic, adipic and other currently used acids, produced from fossil-based resources [14].

Ruthenium-based catalysts are generally known for their aptitude in aerobic oxidation reactions [15–17] including applications for oxidation of alcohols to produce aldehydes or ketones. Hence, homogeneous Ru-complex catalysts have been found to generate aldehydes or ketones in almost quantitative yields when employed in organic solvents [18, 19] or ionic liquids [20]. A more preferred way to oxidize HMF involves heterogeneous catalysis, due to ease of catalyst separation in possible industrial processes [1]. Accordingly, supported ruthenium hydroxide catalysts have recently been reported to be efficient catalysts for aerobic oxidation reactions. $Ru(OH)_x$ supported on ceria has been shown to oxidize alcohols to the corresponding ketones, aldehydes and acids, and also aldehydes to acids with high yields at 80–140 °C at ambient air pressure [21], whereas a $Co(OH)_2$ co-promoted catalyst afforded high activity even at room temperature [22]. Kozhevnikov et al. [23] performed oxidation of primary alcohols to aldehydes using mixed Ru-Co oxide with 95% yield in toluene at 110 °C under oxygen atmosphere. Similarly, a ruthenium-functionalized nickel hydroxide composite catalyst

Electronic supplementary material The online version of this article (doi:10.1007/s10562-011-0707-y) contains supplementary material, which is available to authorized users.

Y. Y. Gorbanev · S. Kegnæs · A. Riisager (✉)
Centre for Catalysis and Sustainable Chemistry, Department of Chemistry, Technical University of Denmark, DK-2800 Kgs. Lyngby, Denmark
e-mail: ar@kemi.dtu.dk

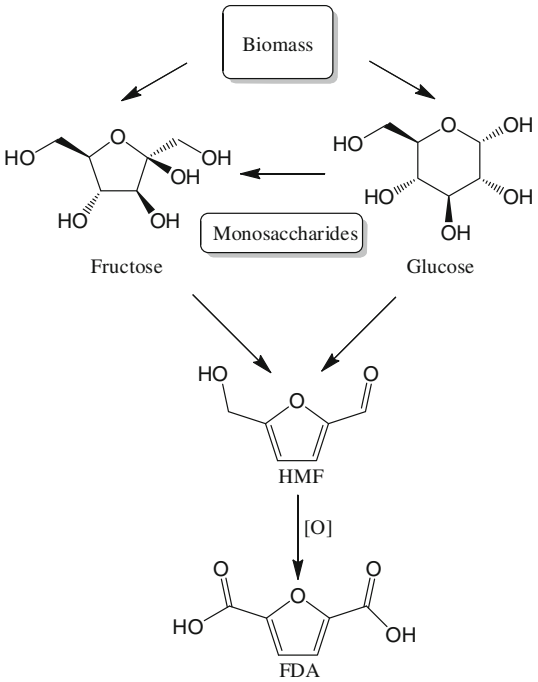

Scheme 1 The schematic route for biomass conversion to FDA

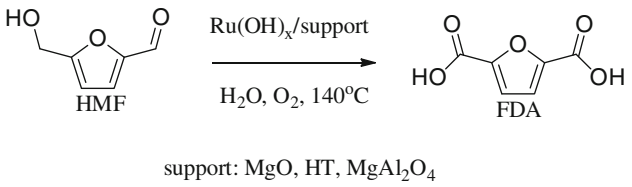

Scheme 2 Aerobic oxidation of HMF to FDA with supported $Ru(OH)_x$ catalyst in water

$(Ru/Ni(OH)_2)$ has been used to oxidize alcohols quantitatively to aldehydes or ketones in organic solvents at 90 °C in the presence of molecular oxygen [24].

Additionally, Kaneda and coworkers [25, 26] and Mizuno and coworkers [27–31] have reported selective aerobic oxidations of aromatic and aliphatic alcohols to aldehydes and ketones and amines to amides with $Ru(OH)_x$ supported by alumina, magnetite and hydroxyapatite. Alcohols and amines were oxidized to produce aldehydes/ketones and amides/nitriles, respectively, at 80–150 °C under ambient pressure of O_2 in toluene or $PhCF_3$ with yield above 99%. Furthermore, alumina-supported ruthenium hydroxide have been used for oxidation of alcohols in a continuous multifunctional reactor [32].

Catalyst supports with basic functionality such as, e.g. hydrotalcite (HT) and hydroxyapatite have also been investigated [29, 30]. Synthetic Ru–Co–Al and Ru–Al–Mg HTs have been reported to catalyze aerobic oxidation of aliphatic and aromatic alcohols in toluene at 60 °C under ambient dioxygen pressure, producing aldehydes and ketones in above 90% yield [33, 34]. Ruthenium- and ruthenium-cobalt-promoted hydroxyapatite gave yields higher than 99% [35, 36].

Recently, we have screened and obtained promising results for the oxidation of HMF with ruthenium hydroxide catalysts on various common supports such as, e.g. magnesium oxide and CeO_2 [37]. In this work we have elaborated the study and investigated the selective oxidation of HMF to FDA with solid catalysts containing $Ru(OH)_x$ species supported on the porous magnesium-containing supports: MgO, spinel and HT (Scheme 2). The reactions were conducted in water with molecular oxygen as the oxidizing agent as a cheap and abundant resource. The catalysts were characterized and the effect of reaction time, pressure and temperature on the catalytic performance were studied and optimized to obtain near quantitative yield of FDA.

2 Experimental

2.1 Materials

HMF (>99%, Sigma-Aldrich), 2-furoic acid (98%, Sigma-Aldrich), levulinic acid (98%, Sigma-Aldrich), formic acid (FA) (98%, Sigma-Aldrich), ruthenium(III) chloride (purum, Sigma-Aldrich), hydrotalcite $Mg_6Al_2(CO_3)(OH)_{16}\cdot 4H_2O$ (HT) and spinel $MgAl_2O_4$ (purum, Sigma-Aldrich), sodium hydroxide (>98%, Sigma-Aldrich), MgO (p.a., Riedel-de Haën AG), DFF (98%, ABCR GmbH & Co.KG), FDA (>99%, Toronto Research Chemicals Inc.), 5-hydroxymethyl-2-furancarboxylic acid (HMFCA) (>99%, Toronto Research Chemicals Inc.) and dioxygen (99.5%, Air Liquide Denmark) were all used as received.

2.2 Catalyst Preparation and Characterization

4.88 g of support (i.e. MgO, $MgAl_2O_4$ or HT) were added to 143 mL of 8.3 mM aqueous $RuCl_3$ solution (1.19 mmol Ru). After stirring for 15 min, 28 mL of 1 M NaOH solution was added and the mixtures were stirred for 18 h. Then the catalysts were filtered off, washed thoroughly with water until the filtrates were neutral (colorless filtrates suggested absence of ruthenium ions) and dried at 140 °C for 40 h. Approximately 4.9 g of each catalyst was obtained containing 2.4 wt% Ru.

XRPD patterns were recorded using a Huber G670 powder diffractometer (Cu-K_α radiation, $\lambda = 1.54056$ Å) in the 2θ interval 5–100°.

Surface areas were determined by nitrogen adsorption and desorption measurements at liquid nitrogen temperature on a Micrometrics ASAP 2020. The samples were

outgased in vacuum at 100 °C for 4 h prior to measurements. The total surface areas were calculated according to the BET method.

TEM images were recorded on a FEI Tecnai Transition Electron Microscope at 200 kV with samples deposited on a carbon support. EDS analysis was performed with an Oxford INCA system.

2.3 Oxidation Reactions

Oxidations were carried out in stirred Parr mini-reactor autoclaves equipped with internal thermocontrol (T316 steel, Teflon™ beaker insert, 100 mL). In each reaction the autoclave was charged with 63 mg of HMF (0.5 mmol) and 10 mL of water. The initial HMF concentration (0.05 M) was chosen based on experimental data on FDA solubility in water and extrapolation of this data to 140 °C. Subsequently, the supported 2.4 wt% $Ru(OH)_x$ catalyst was added (0.105 g, 0.025 mmol Ru). The autoclave was flushed and pressurized with dioxygen (1–40 bar, ca. 1.6–64 mmol) and maintained at 140 °C for a given period of time under stirring (700 rpm). After the reaction, the autoclave was rapidly cooled with ice to room temperature. The reaction mixture was made alkaline with 1 mL of 1 M NaOH solution before filtering off the catalyst, or filtered directly without base, followed by analysis using HPLC (Agilent Technologies 1200 series, Aminex HPX-87H column from Bio-Rad, 300 mm × 7.8 mm × 9 µm, flow 0.6 mL/min, solvent 5 mM H_2SO_4, temperature 60 °C). In all figures where the product distribution is shown as a function of time each data point corresponds to an individual reaction run.

ICP analysis (Perkin Elmer ELAN 6000 with cross-flow nebulizer and argon plasma) was performed on diluted post-reaction mixtures and quantified with ICP standard solutions.

3 Results and Discussion

3.1 Catalyst Characterization

The BET surface areas of the applied support materials and the prepared catalysts are listed in Table 1. The surface areas of the catalysts were very much dependent on the choice of the metal oxide and, as expected, a small decrease in the surface areas was observed between the pure supports and the final catalysts. Moreover, X-ray powder diffraction (XRPD) patterns of the supported catalysts (not shown) revealed exclusively peaks originating from the respective supports, since the ruthenium content on the catalysts was too low to allow detection.

Representative transmission electron microscopy (TEM) images of the prepared catalysts are presented in Fig. 1.

Table 1 Characteristics of supports and supported $Ru(OH)_x$ catalysts

Material	BET surface area (m^2/g)	Ru content (wt%)[a]
MgO	30	–
$Ru(OH)_x$/MgO	27	0.75 (1), 2.48 (2)
$MgAl_2O_4$	63	–
$Ru(OH)_x/MgAl_2O_4$	53	2.41 (1), 2.42 (2)
HT	8	–
$Ru(OH)_x$/HT	6	0.25 (1), 7.55 (2)

[a] The Ru contents are based on Ru:Al atomic ratios provided by EDS. The values of (1) and (2) are related to the areas numbered 1 and 2 on Fig. 1 for the respective support

Notably, only agglomerated crystallites of the respective supports were observed on the TEM images with no noticeable ruthenium particles even at higher resolution. EDS analysis of the catalyst samples (performed on the parts shown in white circles) revealed an uneven distribution of ruthenium species on the surfaces of the catalysts with highest basicity, i.e. MgO and HT. The measured Ru contents are compiled in Table 1.

3.2 Aerobic Oxidation of HMF

Initially, the catalyzed oxidation of HMF to FDA was investigated with $Ru(OH)_x$/HT catalyst in water in the absence of added base at 1 bar dioxygen pressure and a reaction temperature of 140 °C. In Fig. 2 the formation of products is shown as a function of reaction time.

As seen in the figure, HMF was fully converted after 26 h of reaction and a quantitative yield of FDA was obtained after a reaction time of 38 h. Importantly, no product degradation was observed during the examined time period. Two intermediate oxidation products were observed; DFF and HMFCA, thus suggesting a competitive reaction pathway for HMF oxidation with intermediate products formation followed by oxidation to FDA (Scheme 3). This pathway is similar to the route previously established for the gold-catalyzed conversion of HMF [10, 11]. However, the rates of formation and subsequent oxidation of HMFCA and DFF appeared here to be more comparable, though with initial faster formation of DFF under the applied reaction conditions (i.e., 140 °C and 1 bar of O_2 pressure).

Figure 3 shows the distribution of oxidation products obtained after oxidation of HMF for 1 h with $Ru(OH)_x$/HT catalyst at oxygen pressures of 1–40 bar and constant reaction temperature of 140 °C. As shown in the figure, it proved possible to get full conversion of HMF within 1 h by increasing the pressure of oxygen. Moreover, it is evident from the low pressure results that the oxygen pressure

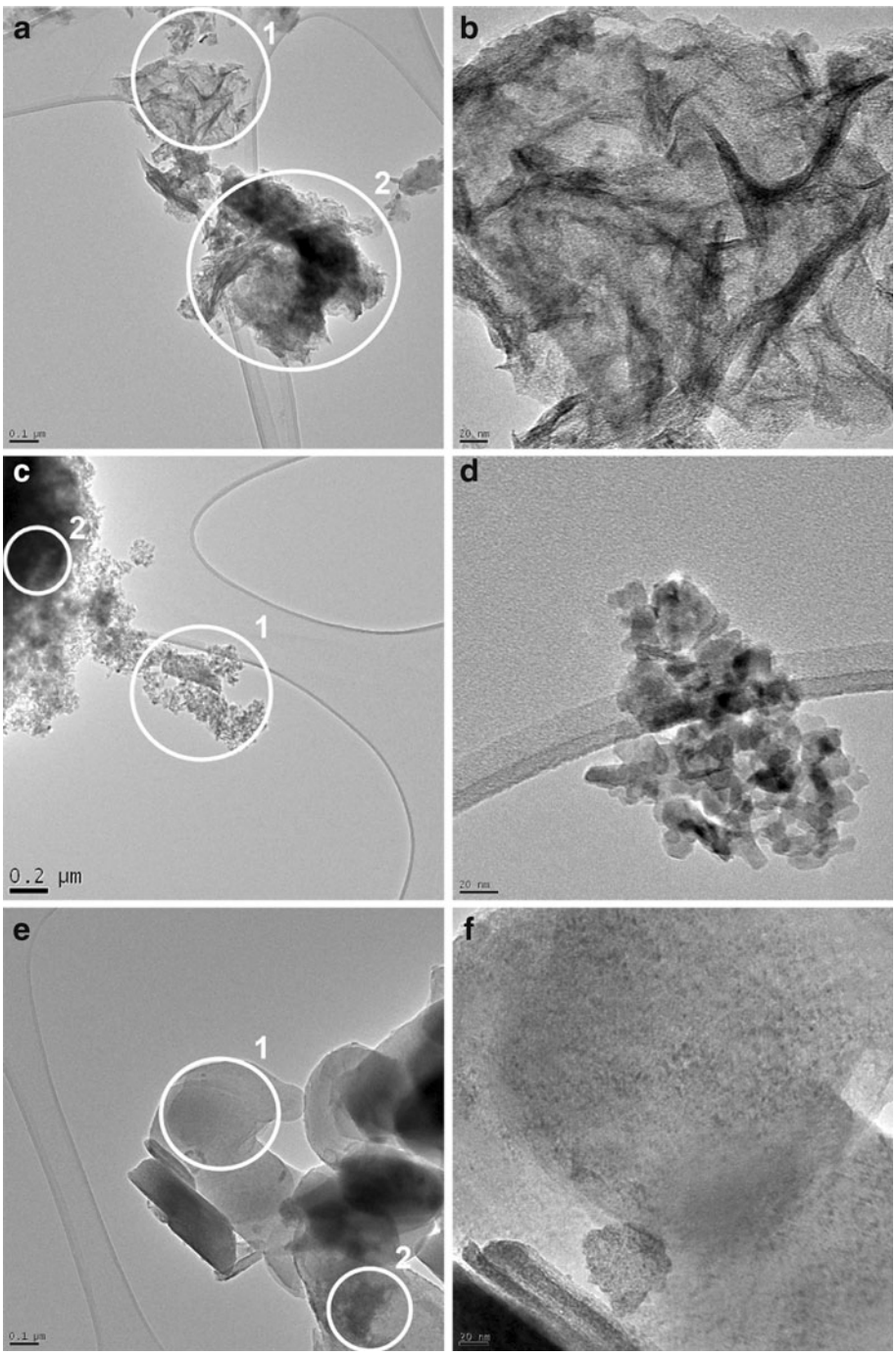

Fig. 1 TEM images of $Ru(OH)_x/MgO$ (**a**, **b**), $Ru(OH)_x/MgAl_2O_4$ (**c**, **d**), and $Ru(OH)_x$/HT (**e**, **f**) catalysts. *White circles* represent the areas analyzed by EDS

dependence was larger on DFF formation than on HMFCA formation (i.e. higher reaction order of oxygen in the rate expression for DFF formation), resulting in a higher rate of oxidation of the alcohol moiety on HMF compared to the aldehyde group. When performing the reaction at 2.5 bar for 1 h it proved therefore possible to form DFF with a relatively high selectivity of about 75%.

In order to elucidate the temperature effect on product formation, a series of experiments were performed with $Ru(OH)_x$/HT catalyst with a reaction time of 6 h and 2.5 bar of oxygen at different reaction temperatures (Fig. 4). The reaction temperature drastically affected the performance of the catalyst which converted essentially all the HMF within 6 h at 100 °C and above. The major product formed at 100 °C was HMFCA (about 80%, with a selectivity of ~85%) while only low amounts of FDA and DFF were formed (5–8%). However, at higher temperatures only FDA was observed giving almost quantitative yield at 140 °C. The absence of DFF after 6 h of reaction time is most likely a result of easier oxidation of the aldehyde functionality [38].

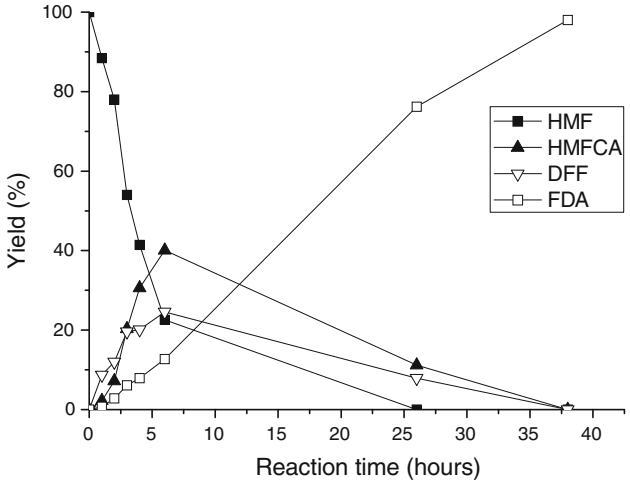

Fig. 2 Product yields in HMF oxidation with $Ru(OH)_x$/HT catalyst in water (0.05 M HMF, 1 bar O_2, 140 °C, 5 mol% Ru to HMF)

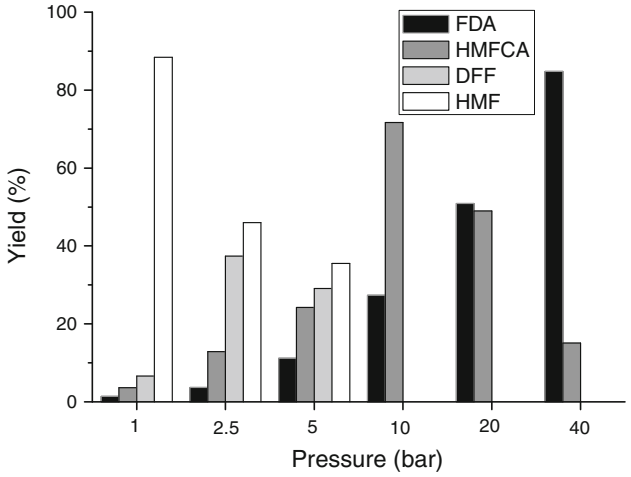

Fig. 3 Product yields in HMF oxidation with $Ru(OH)_x$/HT catalyst in water (0.05 M HMF, 1 h, 140 °C, 5 mol% Ru to HMF)

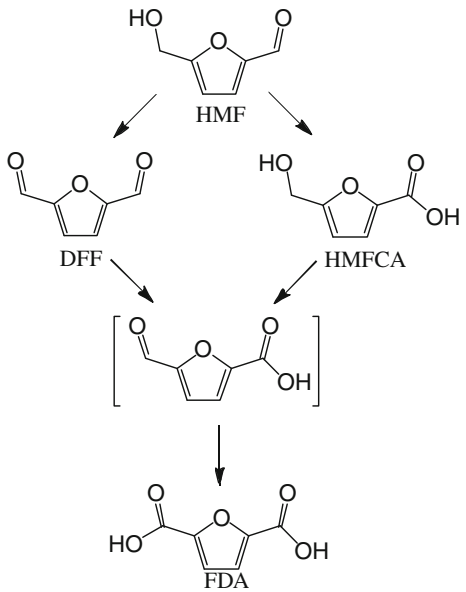

Scheme 3 Reaction pathway from HMF to FDA by aerobic oxidation via the competitive formation of the two intermediate products DFF and HMFCA

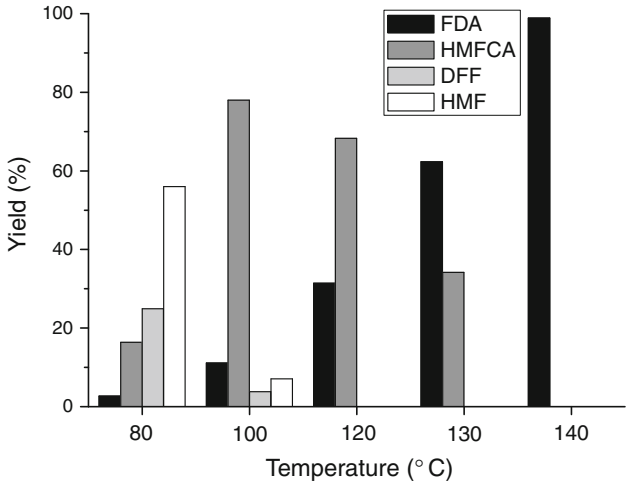

Fig. 4 Product yields in HMF oxidation with $Ru(OH)_x$/HT catalyst in water (0.05 M HMF, 6 h, 2.5 bar O_2, 5 mol% Ru to HMF)

The stability of HMF under the applied reaction conditions was confirmed by conducting an experiment with pure HT support. Here HMF remained essentially unconverted with only ca. 2% of HMF being oxidized and converted to HMFCA (1.3%) and FDA (0.7%), respectively.

To examine the effect of the support on the catalytic activity for the ruthenium-catalyzed conversion of HMF to FDA, catalysts with the alternative magnesium supports, MgO and $MgAl_2O_4$, were also prepared and tested in the oxidation reaction (characteristics of the supports and catalysts are shown in Table 1). The performance of the catalysts were tested under 2.5 bar of oxygen and 140 °C, which was shown to be optimal reactions conditions for the HT supported catalyst (see Fig. 4). The obtained product yields as a function of reaction time are presented in Fig. 5a–c.

The results in Fig. 5 demonstrate that $Ru(OH)_x$ supported on MgO or HT under the applied reaction conditions was able to convert almost all of HMF to FDA, as expected. However, for the $Ru(OH)_x/MgAl_2O_4$ catalyst (Fig. 5c) the activity was lower, resulting in a yield of 60% of FDA after 42 h. Furthermore, a substantial amount (35%) of FA was formed after 42 h with this catalyst. FA, in accordance with literature, may originate from degradation of HMF and FDA [39]. Interestingly, no degradation products were observed when the more alkaline supports MgO and HT were used. Recently, Corma and co-workers reported that usage of ceria-supported gold catalyst in

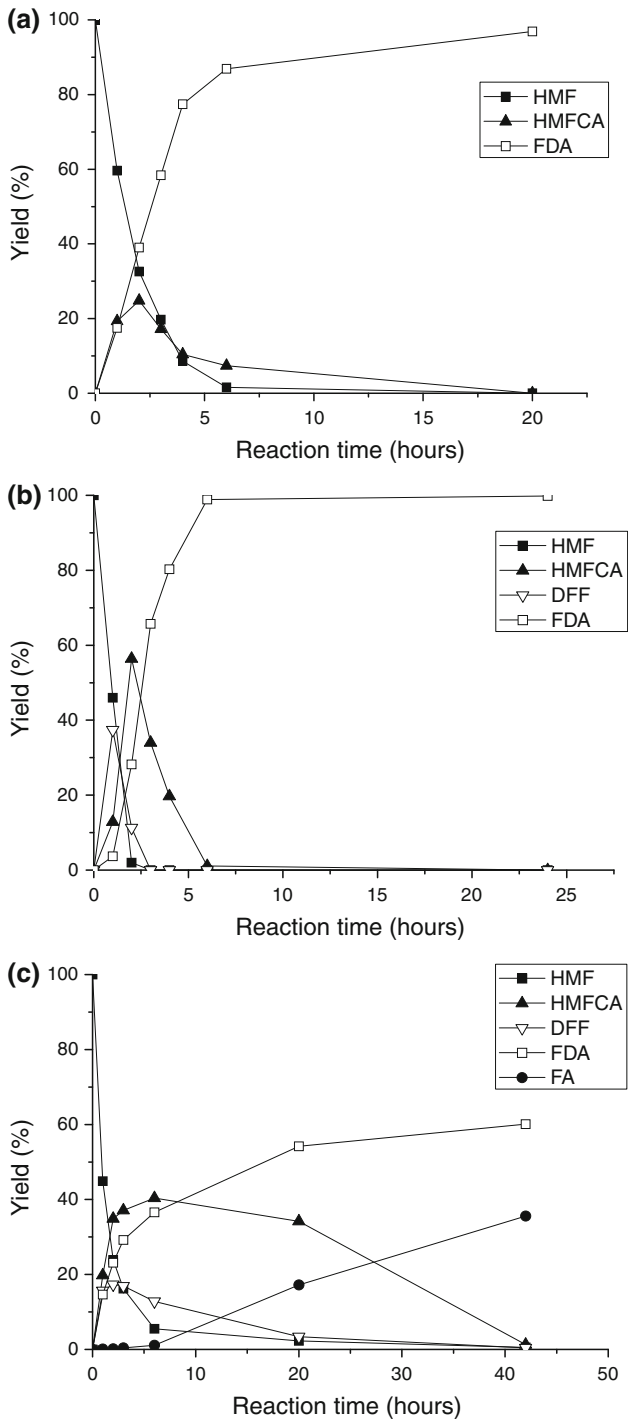

Fig. 5 Product yields in HMF oxidation with $Ru(OH)_x$ catalysts in water supported on **a** MgO, **b** HT or **c** $MgAl_2O_4$ (0.05 M HMF, 2.5 bar O_2, 140 °C, 5 mol% Ru to HMF)

HMF oxidation in alkaline aqueous media led to formation of both ring-opening degradation products and 2-furoic acid [40].

To increase the yield of FDA and limit the formation of FA when using $Ru(OH)_x/MgAl_2O_4$, the effect of oxygen pressure on the HMF oxidation was further investigated. Reactions were performed at 140 °C with a reaction time of 1 h (Fig. 6).

Using the $Ru(OH)_x/MgAl_2O_4$ catalyst the yield of HMFCA and FDA increased when the oxygen pressure was increased, especially up to 5 bar as also found for the $Ru(OH)_x$/HT catalyst (see Fig. 3). Notably, however, an increase in dioxygen pressure from 1 to 2.5 bars resulted in significantly lower formation of FA—from 15 to 0.1%. Based on this observation, the time dependence experiment with the spinel-based catalyst was redone at 5 bar (Fig. 7) instead of 2.5 bar (see Fig. 5c) in order to minimize the byproduct.

From Figs. 5c, and 7 it is clear that at both 2.5 and 5 bar of dioxygen pressure FA formation initiated as the reaction progressed and high relative concentration of the products (i.e. HMFCA, DFF and FDA) accumulated. This indicated that a gradual increase in acidity of the media due to FDA formation could induce furan cycle decomposition. To understand these results in more detail, a control experiment with only $Ru(OH)_x/MgAl_2O_4$ catalyst and FDA (10 mL H_2O, 0.078 g (0.5 mmol) FDA, 2.5 bar O_2, 140 °C, 16 h) was performed to test the stability of FDA in the presence of the catalyst. The experiment revealed that 78% of the initial amount of FDA remained unconverted after the 16 h of reaction whereas partial degradation led to formation of 18% FA. This clearly established the FA—at least partially—to originate from FDA, and possibly also from HMF or the intermediate products HMFCA and DFF. Accordingly, it is possible to limit the formation of FA in the reaction when using $Ru(OH)_x/MgAl_2O_4$ catalyst by applying short reaction time and high relative oxygen pressure.

Application of different magnesium-containing supports resulted in different amounts and distributions of products (see Fig. 5a–c). To understand this difference post-reaction solutions from experiments with each of the catalysts were

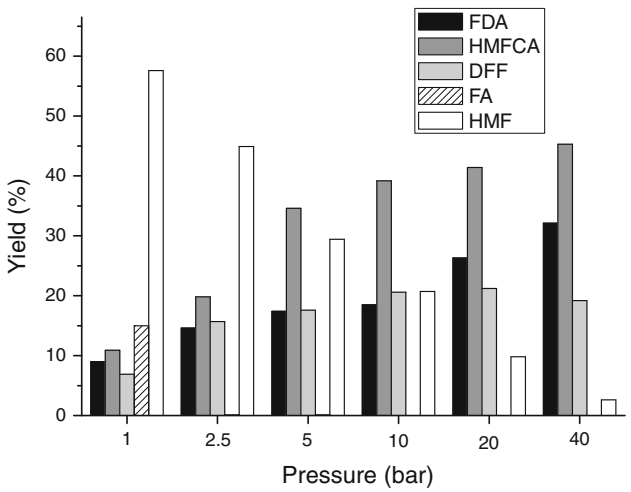

Fig. 6 Product yields in HMF oxidation with $Ru(OH)_x/MgAl_2O_4$ catalyst in water (0.05 M HMF, 1 h, 140 °C, 5 mol% Ru to HMF)

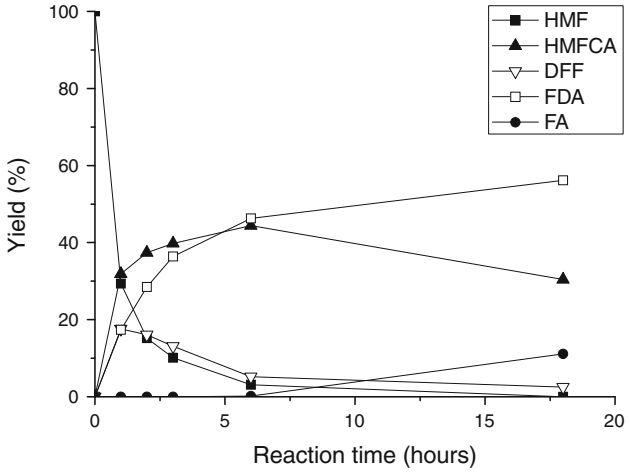

Fig. 7 Product yields in HMF oxidation with $Ru(OH)_x/MgAl_2O_4$ catalyst in water (0.05 M HMF, 5 bar O_2, 140 °C, 5 mol% Ru to HMF)

analyzed by ICP for magnesium and ruthenium content (Table 2).

The ICP analysis confirmed presence of magnesium ions in all post-reaction solutions. Especially, for the HT- and MgO-supported catalysts (Table 2, entries 1 and 2) the amount of leached magnesium was high (26–38%). Notably, the concentration of Mg^{2+}-ions leached from the HT-supported catalyst corresponded to about the amount (i.e. concentration) of FDA formed, thus indicating that the HT support acted as a solid base in the reaction and ionized the FDA to form a Mg-salt which most likely proved more stable towards degradation. Single crystal XRD analysis of the isolated Mg-FDA has recently been reported [41]. Interestingly, HT-supported gold nanoparticle catalyst was, in contrast, recently reported to be reusable and apparently stable in the oxidation of HMF in water under ambient oxygen pressure and elevated temperature [42].

For the MgO support a similar tendency was also observed. The fact that HT dissolved during reaction and neutralized some of the formed FDA also explains the otherwise unexpected neutral pH value measured of the post-reaction solution. Similarly, the high pH value of 10 in the post-reaction solution with MgO support can be associated to its enhanced dissolution under the reaction conditions (Table 2, entry 2).

As the basicity of the respective support decreases in the order MgO > HT > $MgAl_2O_4$ [43], the absence of the DFF product in the HMF oxidation reaction with MgO support (Fig. 5a) might be further explained by the highly basic media (Table 2), possibly facilitating Cannizzaro reaction of the dialdehyde.

In contrast to the HT and MgO supports, the spinel support remained significantly more stable under the reaction conditions permitting only a small amount (0.9%) of the magnesium to dissolve in the acidic post-reaction solution. Accordingly, the formation of FA when using $MgAl_2O_4$ support can be rationalized to be related to lower stability and higher degradation of FDA and HMF in acidic media. In line with this, no degradation of substrate were observed in reactions with catalysts based on the HT and MgO supports, since the solutions here were maintained at high pH throughout the reactions due to partial dissolution of the supports. Additionally, the results of the XRPD analysis did not reveal any change in the spinel structure before and after its employment in the reaction (see Supplementary information, Fig. S1).

In Table 2 the measured amounts of ruthenium in the post-reaction solutions are also reported. Importantly, only an extremely small amount (0.01–0.02%) of the ruthenium metal on the catalysts was dissolved in the examined post-reaction solutions, thus making especially the $Ru(OH)_x/MgAl_2O_4$ catalyst prone for re-use. Hence, an experiment was performed where this catalyst was recovered by filtration, washed with base and water (to remove any FDA

Table 2 ICP analysis of the post-reaction solutions from the aerobic HMF oxidation using supported $Ru(OH)_x$ catalysts (0.05 M HMF, 2.5 bar O_2, 140 °C, 5 mol% Ru to HMF)

Entry	Support	$[Mg^{2+}]$ (g/L)	Mg dissolved (%)[c]	$[Ru^{n+}]$ (mg/L)	Ru dissolved (%)[c]	pH[d]
1[a]	HT	0.980	26	0.030	0.013	7
2[a]	MgO	1.590	38	0.035	0.015	10
3[b]	$MgAl_2O_4$	0.157	0.9	0.046	0.020	2

[a] Measured after 6 h of reaction

[b] Measured after 42 h of reaction

[c] Based on the overall element loading

[d] Measured pH values of the post-reaction solutions

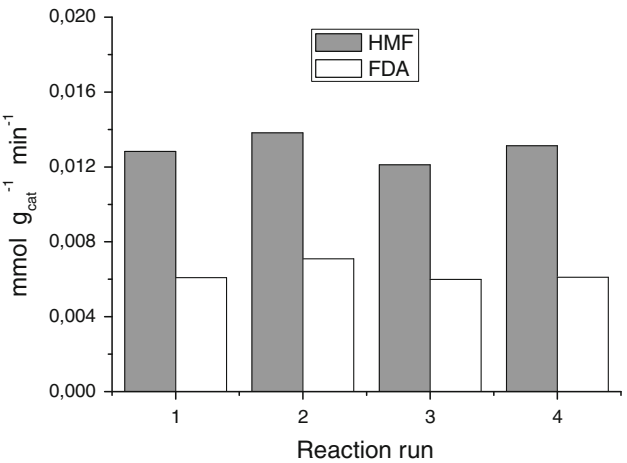

Fig. 8 Rates of HMF conversion and FDA formation per gram of the catalyst in the recycling of $Ru(OH)_x/MgAl_2O_4$ catalyst in water (0.05 M HMF, 5 bar O_2, 140 °C, 5 mol% Ru to HMF, 6 h of reaction time)

precipitated on the surface of the catalyst after cooling down the reaction mixture) and re-used (Fig. 8). As seen from the results, the spinel-supported ruthenium catalyst preserved its initial activity clearly making this stable heterogeneous $Ru(OH)_x$ oxidation catalyst interesting for further investigations.

4 Conclusions

Supported catalysts with catalytically active $Ru(OH)_x$ species deposited on the three magnesium-based supports HT, MgO and spinel ($MgAl_2O_4$), have been applied for aerobic oxidation of HMF to FDA in water without added base. All three catalysts were found to effectively catalyze the oxidation of HMF. However, both HT and MgO supports dissolved partly under the reaction conditions liberating significantly amounts of Mg^{2+} ions, thus making the mixtures alkaline. This resulted in formation of Mg-FDA salts stabilized against further degradation. The spinel support, on the other hand, remained stable under the reaction conditions which allowed performing the oxidation reaction under base free conditions.

The reported data suggests that the reaction pathway for aerobic oxidation of HMF to FDA with the $Ru(OH)_x$ supported catalysts proceed via relatively slow initial competitive oxidation to DFF and HMFCA (Scheme 3). The subsequent oxidations to form the product are fast since no other intermediates (e.g. 5-formylfuran-2-carboxylic acid) were observed.

Importantly, only very low amounts (<0.02%) of the ruthenium metal inventory was found to dissolve from the catalysts (irrespectively of the support dissolution) under the applied reaction conditions. Combined with the observation that $Ru(OH)_x/MgAl_2O_4$ preserved its activity upon reuse, makes this and analogous catalyst systems based on stable supports attractive alternatives to present aerobic HMF oxidation catalysts based on metal nanoparticles (e.g. gold catalysts), which often is less active upon reuse due to particle sintering [10, 44].

Acknowledgments The authors thank Bodil Holten (Centre for Catalysis and Sustainable Chemistry, DTU Chemistry) for experimental assistance. The work was supported by The Danish National Advanced Technology Foundation and Novozymes A/S.

References

1. Rinaldi R, Schüth F (2009) Energy Environ Sci 2:610
2. Park J, Seyama T, Shiroma R, Ike M, Srichuwong S, Nagata K, Arai Sanoh Y, Kondo M, Tokuyasu K (2009) Biosci Biotechnol Biochem 73:1072
3. Schäfer T, Borchert TW, Nielsen VS, Skagerlind P, Gibson K, Wenger K, Hatzack F, Nilsson LB, Salmon S, Pedersen S, Heldt-Hansen HP, Poulsen PB, Lund H, Oxenbøll KM, Wu GF, Pedersen HH, Xu H (2007) Adv Biochem Eng Biotechnol 105:59
4. Du Z, Ma J, Wang F, Liu J, Xu J (2011) Green Chem 13:554
5. Navarro OC, Canós AC, Chornet SI (2009) Top Catal 52:34
6. Ma J, Du Z, Xu J, Chu Q, Pang Y (2011) ChemSusChem 4:51
7. Grabowski G, Lewkowski J, Skowroński R (1991) Electrochim Acta 36:1995
8. Lilga MA, Hallen RT, Hu J, White JF, Gray MJ (2008) US Patent 20080103318, 1 may 2008
9. Casanova O, Iborra S, Corma A (2009) J Catal 265:109
10. Gorbanev YY, Klitgaard SK, Woodley JM, Christensen CH, Riisager A (2009) ChemSusChem 2:672
11. Taarning E, Nielsen IS, Egeblad K, Madsen R, Christensen CH (2008) ChemSusChem 1:75
12. Werpy T, Petersen G (2004) Top Value Added Chem Biomass 1:26 http://www.osti.gov/bridge
13. Bozell JJ, Petersen GR (2010) Green Chem 12:539
14. Boisen A, Christiansen TB, Fu W, Gorbanev YY, Hansen TS, Jensen JS, Klitgaard SK, Pedersen S, Riisager A, Ståhlberg T, Woodley JM (2009) Chem Eng Res Des 87:1318
15. Dijksman A, Arends IWCE, Sheldon RA (2001) Platinum Metals Rev 45:15
16. Chang S, Lee M, Ko S, Lee PH (2002) Synth Commun 32:1279
17. Vanover E, Huang Y, Xu L, Newcomb M, Zhang R (2010) Org Lett 12:2246
18. Zhai Y, Liu H, Liu B, Liu Y, Xiao J, Bai W (2007) Trans Met Chem 32:570
19. Lei ZQ, Kang QX, Bai XZ, Yang ZW, Zhang QH (2005) Chin Chem Lett 16:846
20. Farmer V, Welton T (2002) Green Chem 4:97
21. Vocanson F, Guo YP, Namy IL, Kagan HB (1998) Synth Commun 28:2577
22. Ji H, Mizugaki T, Ebitani K, Kaneda K (2002) Tetrahedron Lett 43:7179
23. Musawir M, Davey PN, Kelly G, Kozhevnikov IV (2003) Chem Commun 1414
24. Venkatesan S, Kumar AS, Lee J-F, Chan T-S, Zen J-M (2009) Chem Commun 1912
25. Yamaguchi K, Mori K, Mizugaki T, Ebitani K, Kaneda K (2000) J Am Chem Soc 122:7144
26. Mori K, Yamaguchi K, Mizugaki T, Ebitani K, Kaneda K (2001) Chem Commun 461
27. Yamaguchi K, Mizuno N (2003) Chem Eur J 9:4353
28. Kotani M, Koike T, Yamaguchi K, Mizuno N (2006) Green Chem 8:735
29. Kim JW, Yamaguchi K, Mizuno N (2008) Angew Chem Int Ed 47:9249
30. Mizuno N, Yamaguchi K (2008) Catal Today 132:18
31. Yamaguchi K, Mizuno N (2010) Synlett 16:2365
32. Bavykin DV, Lapkin AA, Kolaczkowski ST, Plucinski PK (2005) Appl Catal A 288:175
33. Kaneda K, Yamashita T, Matsushita T, Ebitani K (1998) J Org Chem 63:1750
34. Matsushita T, Ebitani K, Kaneda K (1999) Chem Commun 265
35. Opre Z, Grunwaldt J-D, Maciejewski M, Ferri D, Mallat T, Baiker A (2005) J Catal 230:406
36. Opre Z, Grunwaldt J-D, Mallat T, Baiker A (2005) J Mol Catal A 242:224
37. Gorbanev YY, Kegnæs S, Riisager A (2011) Top Catal. doi: 10.1007/s11244-011-9754-2
38. Marsden C, Taarning E, Hansen D, Johansen L, Klitgaard SK, Egeblad K, Christensen CH (2008) Green Chem 10:168
39. Lewkowski J (2001) ARKIVOC (i) 17–54
40. Casanova O, Iborra S, Corma A (2009) ChemSusChem 2:1138

41. Schau-Magnussen M, Gorbanev YY, Kegnæs S, Riisager A (2011) Acta Cryst C67:m327
42. Gupta NK, Nishimura S, Takagaki A, Ebitani K (2011) Green Chem 11:824
43. Di Cosimo JI, Diez VK, Xu M, Iglesia E, Apesteguia CR (1998) J Catal 178:499
44. Hashmi ASK, Hutchings G (2006) Angew Chem Int Ed 45:7896